

Statistical hadronization of charm in heavy-ion collisions at SPS, RHIC and LHC

A. Andronic^a, P. Braun-Munzinger^a, K. Redlich^{b,c}, J. Stachel^d

^a*Gesellschaft für Schwerionenforschung, GSI,
D-64291 Darmstadt, Germany*

^b*Fakultät für Physik, Universität Bielefeld,
Postfach 100 131, D-33501 Bielefeld, Germany*

^c*Institute of Theoretical Physics, University of Wrocław,
PL-50204 Wrocław, Poland*

^d*Physikalisches Institut der Universität Heidelberg,
D-69120 Heidelberg, Germany*

Abstract

We study the production of charmonia and charmed hadrons in nucleus-nucleus collisions at SPS, RHIC, and LHC energies within the framework of the statistical hadronization model. Results from this model are compared to the measured yields and centrality dependence of J/ψ production at SPS and RHIC energies. We explore and contrast the centrality dependence of the production of mesons with open and hidden charm at SPS, RHIC and LHC. The sensitivity of the results to various input parameters is analyzed in detail for RHIC energy.

Key words: statistical hadronization, open and hidden charm hadrons, J/ψ suppression or enhancement

PACS: 25.75.-q, 25.75.Nq, 25.75.Dw

1 Introduction

The concept of a possible thermal origin of charmonia was initially introduced [1] to explain the measurement of the J/ψ /hadron ratio in nuclear collisions. Because of their large mass and small production cross section at thermal energies charm quarks are, however, not likely to be thermally produced. On the other hand, significant production of charm quark pairs takes place in initial hard collisions. This led to the idea of statistical hadronization of charm quarks [2,3], which has sparked an intense activity in this field [4,5,6,7,8]. At about the same time an independent effort [9,10] based on a kinetic model

has been developed to study charm production in heavy ion collisions at collider energies. Initial interest focussed on the available SPS data on J/ψ production in Pb–Pb collisions. As we stress below, these data can indeed be described within the statistical approach, but only when assuming the charm production cross section to be enhanced beyond the perturbative QCD (pQCD) predictions.

The largest differences between the results of the statistical coalescence scenario and earlier models are expected at collider energies. For example, for central Au–Au collision at RHIC energy, the Satz–Matsui approach [11] predicts a very strong (up to a factor of 20 [12]) suppression of J/ψ yields as compared to a direct production. In the present approach this suppression is overcome by statistical recombination of J/ψ mesons from the initially produced $c\bar{c}$ pairs, so that much larger yields are expected.¹ We therefore focus in this letter on the predictions of the model for open and hidden charm meson yields at RHIC (Au–Au) and LHC (Pb–Pb) energies, with particular emphasis on the centrality dependence of rapidity densities at RHIC. We, furthermore, present predictions for the energy dependence of the production of hadrons with open and hidden charm.

2 Model description and input parameters

The model assumes that all charm quarks are produced in primary hard collisions and equilibrate² in the quark-gluon plasma (QGP). In particular, no J/ψ mesons are pre-formed in the QGP, implying complete color screening [11]. There are indications from recent lattice QCD calculations that, already at SPS energies, J/ψ mesons can be dissociated in a deconfined medium via collisions with thermal gluons [13,14]. As noted earlier [2], the cross sections of charmed hadrons are too small to allow for their chemical equilibration in a hadronic gas. We assume that open and hidden charm hadrons are formed at chemical freeze-out according to statistical laws. Consistent with the fact that, at SPS energy and beyond, chemical freeze-out appears to be at the phase boundary [15], our model implies that a QGP phase was a stage in the evolution of the fireball. The analysis of J/ψ spectra at SPS [16] lends further support to the statistical hadronization picture where J/ψ decouples at chemical freeze-out. A recent analysis of electron spectra at RHIC [17] also strenghtens the case for an early thermalization of heavy quarks. However, in that analysis it was pointed out that both the hydrodynamical approach and PYTHIA reproduce the measured single-electron spectra. As suggested meanwhile [18], the measurement of the elliptic flow (v_2) of open charm hadrons and J/ψ may help to disentangle the two scenarios. Recent work [19] in extracting the quark v_2 from the one of hadrons may help towards this goal. Most important though, in our view, is a high-precision direct measurement of open charm. As expected, and as seen in ref. [17], the p_t spectra predicted by PYTHIA and hydro are different in detail at low p_t and differ manifestly at high p_t ($p_t \gg$ mass of charm quark). On the other hand, a recent theoretical analysis [20]

¹ The absence of J/ψ suppression at RHIC energy is also predicted by the kinetic model [9,10].

² This implies thermal, but not chemical equilibrium for charm quarks.

indicates that charm quarks might not thermalize quickly because of their large mass.

In statistical models charm production needs generally to be treated within the framework of canonical thermodynamics [21]. Thus, the charm balance equation required [2,3] during hadronization is expressed as:

$$N_{c\bar{c}}^{dir} = \frac{1}{2}g_c N_{oc}^{th} \frac{I_1(g_c N_{oc}^{th})}{I_0(g_c N_{oc}^{th})} + g_c^2 N_{c\bar{c}}^{th}. \quad (1)$$

Here $N_{c\bar{c}}^{dir}$ is the number of directly produced $c\bar{c}$ pairs and I_n are modified Bessel functions. In the fireball of volume V the total number of open $N_{oc}^{th} = n_{oc}^{th}V$ and hidden $N_{c\bar{c}}^{th} = n_{c\bar{c}}^{th}V$ charm hadrons are computed from their grand-canonical densities n_{oc}^{th} and $n_{c\bar{c}}^{th}$, respectively. The densities of different particle species in the grand canonical ensemble are calculated following the statistical model introduced in [23]. All known charmed mesons and hyperons and their decays [22] have to be included in the calculations.

The balance equation (1) defines a fugacity parameter g_c that accounts for deviations of charm multiplicity from the value that is expected in complete chemical equilibrium. The yield of open charm mesons and hyperons i and of charmonia j is obtained from:

$$N_i = g_c N_i^{th} \frac{I_1(g_c N_{oc}^{th})}{I_0(g_c N_{oc}^{th})} \quad \text{and} \quad N_j = g_c^2 N_j^{th}. \quad (2)$$

The above model for charm production and hadronization can be only used [2,27] if the number of participating nucleons N_{part} is sufficiently large. Taking into account the measured dependence of the relative yield of ψ' to J/ψ on centrality [25] in Pb–Pb collisions at SPS energy the model appears appropriate [2,27] if $N_{part} > 100$.

To calculate the yields of open and hidden charm hadrons for a given centrality and collision energy one needs to fix a set of parameters in Eq.(1) and (2):

i) A constant temperature of 170 MeV and a baryonic chemical potential μ_b according to the parametrization $\mu_b = 1270[\text{MeV}]/(1 + \sqrt{s_{NN}}[\text{GeV}]/4.3)$ [37] are used for our calculations. For SPS and RHIC energies these thermal parameters are consistent, within statistical errors, with those required to describe experimental data on different hadron yields [23,24]. In Table 1 we present the values of these input parameters and the resulting chemical potentials for isospin, strangeness and charmness for the canonical ensemble calculations at SPS, RHIC and LHC.

ii) The volume of the fireball corresponding to a slice of one rapidity unit at midrapidity, $V_{\Delta y=1}$, is obtained from the charged particle rapidity density dN_{ch}/dy , via the relation $dN_{ch}/dy = n_{ch}^{th} V_{\Delta y=1}$, where n_{ch}^{th} is the charged particle density computed within the thermal model. The charged particle rapidity densities (and total yields in case of SPS) are taken from experiments at SPS [28] and RHIC [29] and extrapolated to LHC energy. In Fig. 1 we show a compilation of experimental data on dN_{ch}/dy at midrapidity for

Table 1

Input values of T and μ_b and output chemical potentials for isospin, strangeness and charmness for canonical ensemble calculations at SPS, RHIC and LHC.

$\sqrt{s_{NN}}$ (GeV)	17.3	200	5500
T (MeV)	170	170	170
μ_b (MeV)	253	27	1
μ_{I_3} (MeV)	-10.1	-0.96	-0.037
μ_S (MeV)	-68.6	6.70	0.304
μ_C (MeV)	-41.8	-3.92	-0.156

central collisions in the energy range from AGS [30] up to RHIC³. The continuous line in Fig. 1 is the prediction [33] of the saturation model, the dashed line is a flatter power law dependence, both arbitrarily normalized. We use the $(\sqrt{s_{NN}})^{0.3}$ dependence of dN_{ch}/dy to get the value of $dN_{ch}/dy \simeq 2000$ for LHC energy. Throughout this paper we define central collisions by the average value $N_{part}=350$, which roughly corresponds to the topmost 5% of the nuclear cross section. For the centrality dependences we assume that the volume of the fireball is proportional to N_{part} .

iii) The yield of open charm $N_{c\bar{c}}^{dir}$ is taken from next-to-leading order (NLO) pQCD calculations for p-p collisions [34] and scaled to nucleus-nucleus collision via the nuclear overlap function [35,36] T_{AA} . For a given centrality: $N_{c\bar{c}}^{dir}(N_{part}) = \sigma(pp \rightarrow c\bar{c})T_{AA}(N_{part})$. The pQCD calculations with the MRST HO parton distribution function (PDF) are used here [34]. We note that the pQCD results, in particular at LHC energy, are sensitive on the choice of PDF and/or charm quark mass value [34].

The input values dN_{ch}/dy and $dN_{c\bar{c}}^{dir}/dy$ and the corresponding volume at midrapidity and enhancement factor are summarized in Table 2 for model calculations for different collision energies.

Table 2

Input (dN_{ch}/dy and $dN_{c\bar{c}}^{dir}/dy$) and output ($V_{\Delta y=1}$ and g_c) parameters for model calculations at top SPS, RHIC and LHC for central collisions.

$\sqrt{s_{NN}}$ (GeV)	17.3	200	5500
dN_{ch}/dy	430	730	2000
$dN_{c\bar{c}}^{dir}/dy$	0.064	1.92	16.8
$V_{\Delta y=1}$ (fm ³)	861	1663	4564
g_c	1.86	8.33	23.2

³ A constant Jacobian of 1.1 has been used to convert the $dN_{ch}/d\eta$ data to dN_{ch}/dy .

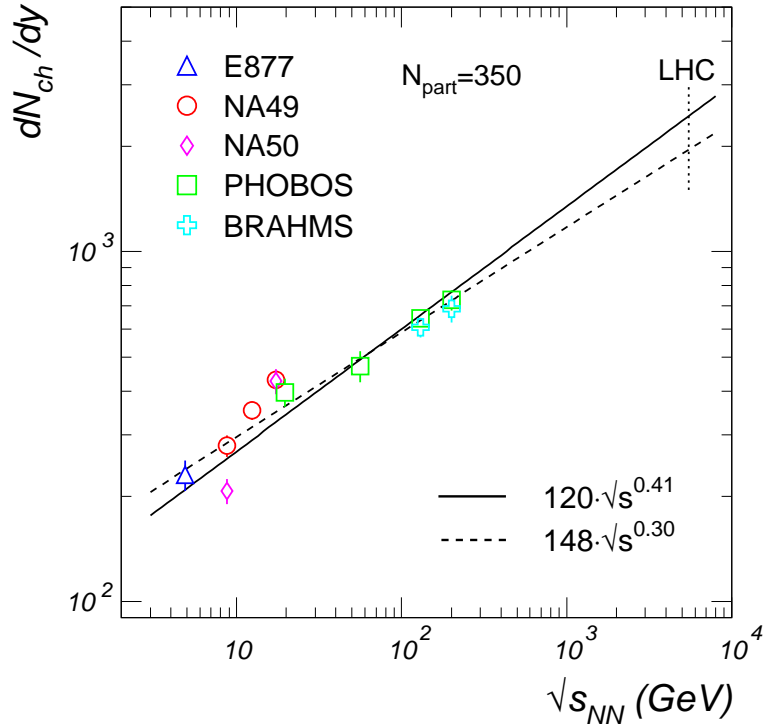


Fig. 1. Experimental values of charged particle yields at midrapidity as a function of collisions energy for central collisions. The data points are from experiments at AGS (E877 [30]), SPS (NA49 [28], NA50 [31]) and RHIC (PHOBOS [29], BRAHMS [32]). The continuous and dashed lines are power law dependences (see text), the dotted line marks the full LHC energy for Pb-Pb collisions ($\sqrt{s_{NN}}=5.5$ TeV).

3 Model results and predictions

We first compare predictions of the model to 4π -integrated J/ψ data at the SPS energy. The NA50 data [38,39] are replotted in Fig. 2 as outlined in [3]. The model results shown in Fig. 2 are going beyond that of [3] since we have included a complete set of charmed mesons and baryons as well as updated the values of the charm production cross section and the volume of the fireball. Recent results [28] of the NA49 Collaboration on total charged particle multiplicity in central collisions yield $N_{ch} = 1533$, leading to a fireball total volume $V=3070$ fm³ and to a corresponding total yield of thermal open charm pairs of $N_{oc}^{th}=0.98$. This is to be contrasted with $N_{cc}^{dir}=0.137$ from NLO calculations [34], leading to a value of $g_c=0.78$. Although g_c is here close to unity, this obviously does not indicate that charm production appears at chemical equilibrium, as the suppression factor is a strongly varying function of the collision energy. We have already indicated that, within the time scales available in heavy ion collisions, the chemical equilibration of charm is very unlikely both in confined and deconfined media [40].

In Fig. 2 we show the comparison between the results of our model and NA50 data for two

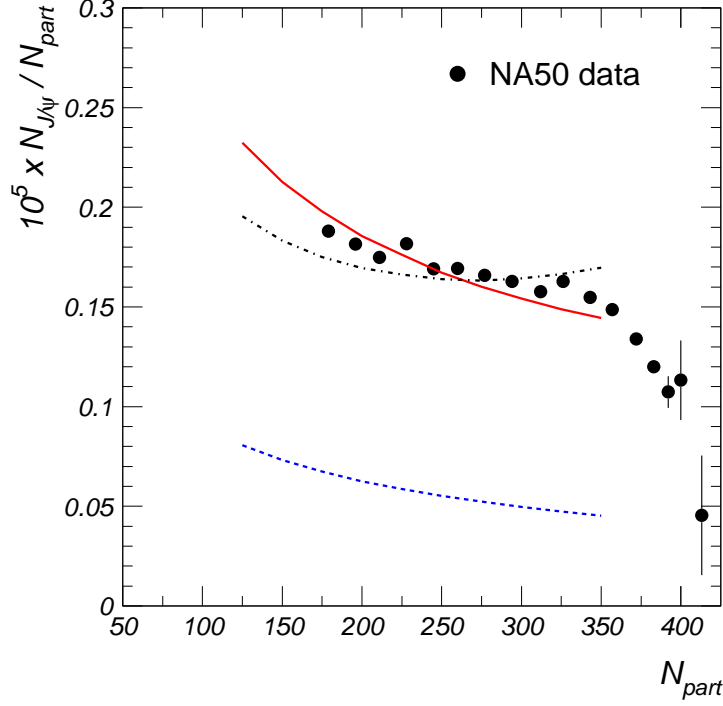


Fig. 2. The centrality dependence of J/ψ production at SPS. Model predictions are compared to 4π -integrated NA50 data [38,39]. Two curves for the model correspond to the values of $N_{c\bar{c}}^{dir}$ from NLO calculations (dashed line) and scaled up by a factor of 2.8 (continuous line). The dash-dotted curve is obtained when considering the possible NA50 N_{part} -dependent charm enhancement over their extracted p-p cross section [41] (see text).

different values of $N_{c\bar{c}}^{dir}$: from NLO calculations [34] and scaled up by a factor of 2.8. Using the NLO cross sections for charm production scaled by the nuclear overlap function, the model underestimates the measured yield. To explain the overall magnitude of the data, one needs to increase the $N_{c\bar{c}}^{dir}$ yield by a factor of 2.8 as compared to NLO calculations. We mention in this context that the observed [41] enhancement of the di-muon yield at intermediate masses has been interpreted as a possible indication for an anomalous increase of the charm production cross section [42]. A third calculation (resulting in the dash-dotted line in Fig. 2) is using the NLO cross section scaled-up by 1.6, which is the ratio of the open charm cross section estimated by NA50 for p-p collisions at 450 GeV/c [41] and the present NLO values. For this case the N_{part} scaling is not the overlap function, but is taken according to the measured di-muon enhancement as a function of N_{part} [41]. The resulting J/ψ yields from the statistical model are on average in agreement with the data, albeit with a flatter centrality dependence than by using the nuclear overlap function. Thus our charm enhancement factor of 2.8 needed to explain the J/ψ data is very similar to the factor needed to explain the intermediate mass dilepton enhancement assuming that it arises exclusively from charm enhancement [41]. We note, however, that other plausible explanations exist of the observed enhancement in terms of thermal radiation [43,44].

The drop of the J/ψ yield per participant observed in the data for $N_{part} > 350$ (see Fig. 2) is currently understood in terms of further J/ψ dissociation due to energy density fluctuations for a given overlap geometry [45]. Alternatively, the drop has been connected with a possible trigger bias in the data [46]. Note that this second drop is only visible in the minimum bias analysis [38]. These aspects are not included in the current model, however when being incorporated the J/ψ yield for very central collisions can be as well reproduced [7,8].

Table 3

Mid-rapidity densities for open and hidden charm hadrons, calculated for central collisions at SPS, RHIC and LHC.

$\sqrt{s_{NN}}$ (GeV)	17.3	200	5500
dN_{D^+}/dy	0.010	0.404	3.56
dN_{D^-}/dy	0.016	0.420	3.53
dN_{D^0}/dy	0.022	0.888	7.80
$dN_{\bar{D}^0}/dy$	0.035	0.928	7.82
$dN_{D_s^+}/dy$	0.012	0.349	2.96
$dN_{D_s^-}/dy$	0.009	0.338	2.95
dN_{Λ_c}/dy	0.014	0.153	1.16
$dN_{\bar{\Lambda}_c}/dy$	0.0012	0.117	1.15
$dN_{J/\psi}/dy$	$2.55 \cdot 10^{-4}$	0.011	0.226
$dN_{\psi'}/dy$	$0.95 \cdot 10^{-5}$	$3.97 \cdot 10^{-4}$	$8.46 \cdot 10^{-3}$

We turn now to discuss our model predictions for charmonia and open charm production at collider energies and compare them with the results obtained at SPS. Notice that from now on we focus on rapidity densities, which are the relevant observables at the colliders. In Table 3 we summarize the yields for a selection of hadrons with open and hidden charm. All predicted yields increase strongly with beam energy, reflecting the increased charm cross section and the concomitant importance of statistical recombination. Also, ratios of open charm hadrons evolve with increasing energy, reflecting the corresponding decrease in the charm chemical potential.

Model predictions for the centrality dependence of J/ψ and D^+ rapidity densities normalized to N_{part} are shown in Fig. 3. The results for J/ψ mesons exhibit, in addition to the dramatic change in magnitude, a striking change in the shape of the centrality dependence. In terms of the model this change is a consequence of the transition from the canonical to the grand-canonical regime [3]. For D^+ -mesons, the expected approximate scaling of the ratio $D^+/N_{part} \propto N_{part}^{1/3}$ (dashed lines in Fig. 3) is only roughly fulfilled due to departures of the nuclear overlap function from the simple $N_{part}^{4/3}$ dependence.

The results summarized in Table 3 and shown in Fig. 3 obviously depend on two input parameters, dN_{ch}/dy and dN_{cc}^{dir}/dy . For LHC energy, neither one of these parameters is

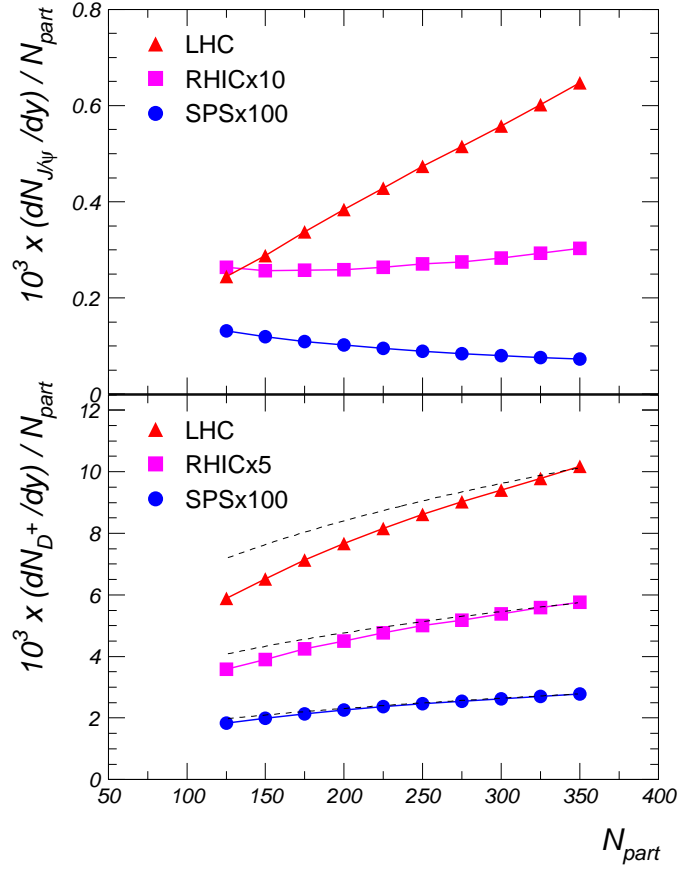


Fig. 3. Centrality dependence of rapidity densities of J/ψ (upper panel) and D^+ (lower panel) mesons per participant at SPS, RHIC and LHC. Note the scale factors for RHIC and SPS energies. The dashed lines in the lower panel represent $N_{part}^{1/3}$ dependences normalized for $N_{part}=350$.

well known. An increase of charged particle multiplicities by up to a factor of three beyond our “nominal” value $dN_{ch}/dy=2000$ for central collisions is conceivable. The saturation model, e.g., leads to a prediction of [33] $dN_{ch}/dy \simeq 2300$. However, due to quite large uncertainties on the amount of shadowing at LHC energy, these results may be still modified. The yield of dN_{cc}^{dir}/dy is also not well known at LHC energy. Although these uncertainties affect considerably the magnitude of the predicted yields, their centrality dependence remains qualitatively unchanged: the yields per participant are increasing functions of N_{part} . We also note here that, while detailed predictions differ significantly, qualitatively similar results (see ref. [47]) have been obtained for a kinetic model study of J/ψ production at the LHC.

In Fig. 4 we present the predicted centrality dependence of the J/ψ rapidity density normalized to N_{part} for RHIC energy ($\sqrt{s_{NN}}=200$ GeV). The three panels show its sensitivity on dN_{ch}/dy , dN_{cc}^{dir}/dy , and (freeze-out) temperature T . The calculations are compared to experimental results of the PHENIX Collaboration [48]. Note that the point for the central collisions is the upper limit extracted by PHENIX for 90% C.L. [48]. The experimental data have been rescaled according to our procedure [36] to calculate N_{part} and the number of binary collisions, N_{coll} . Using the centrality intervals of PHENIX, we obtain

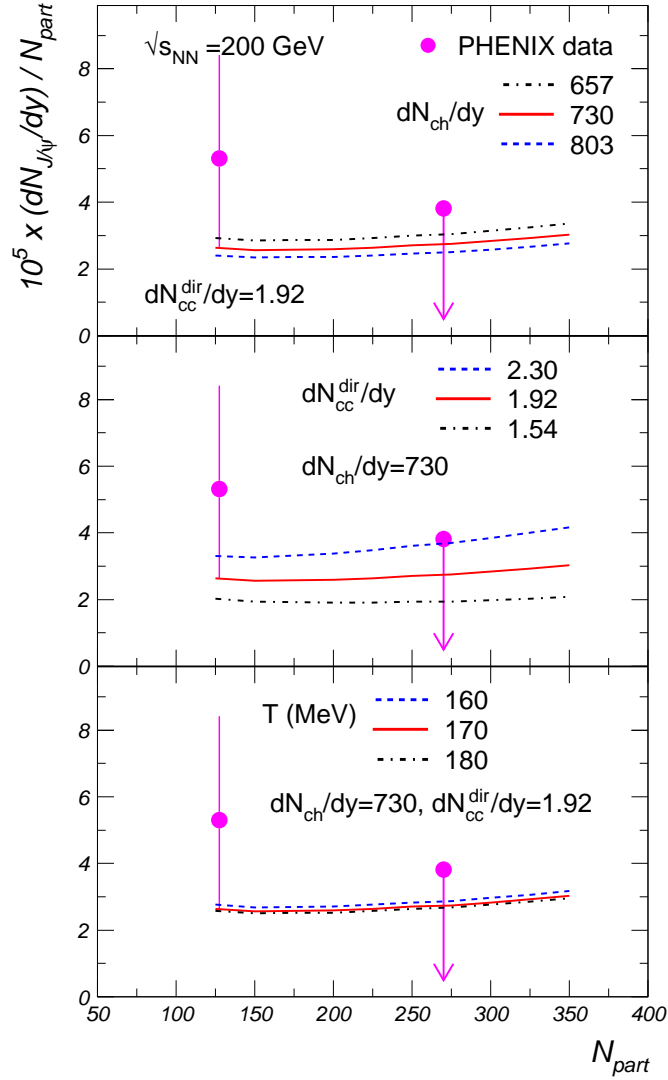


Fig. 4. Centrality dependence of rapidity densities of J/ψ mesons at RHIC. Upper panel: sensitivity to dN_{ch}/dy ; middle panel: sensitivity to dN_{cc}^{dir}/dy ; lower panel: sensitivity to T . The calculations are represented by lines. The dots are experimental data from the PHENIX collaboration [48]. Note that the point for the central collisions is the upper limit extracted by PHENIX for 90% C.L. [48].

$N_{coll} = 275$ and 782 (the differences to the PHENIX values of 296 and 779, respectively, are small). We use $\sigma_{NN}=42$ mb and a Woods-Saxon density profile.

Within the still large experimental error bars, the measurements agree with our model predictions. In Fig. 4 only the statistical errors of the mid-central data point are plotted. The systematic errors are also large [48]. peripheral collisions. A stringent test of the present model can only be made when high statistics J/ψ data are available. In any case, very large J/ψ suppression factors as predicted, e.g., by [12] seem to be not supported by the data.

We turn now to a more detailed discussion of the sensitivity of our calculations to the various input parameters as quantified in Fig. 4. First we consider the influence of a 10% variation of dN_{ch}/dy on the centrality dependence of J/ψ yield. Note that the total experimental uncertainty of $dN_{ch}/d\eta$ (which is for the moment the measured observable for most experiments) at RHIC is below 10% [29,32]. The sensitivity on the dN_{ch}/dy values stems from the volume into which the (fixed) initial number of charm quarks is distributed. The smaller the particle multiplicities and thus also the fireball volume, the more probable it is for charm quarks and antiquarks to combine and form quarkonia. That is why one sees, in the top panel in Fig. 4, that the J/ψ yield is increasing with decreasing charge particle multiplicity.

The sensitivity of the predicted J/ψ yields on $dN_{c\bar{c}}^{dir}/dy$ is also straightforward. The larger this number is in a fixed volume the larger is the yield of charmed hadrons. In case of charmonia the dependence on $dN_{c\bar{c}}^{dir}/dy$ is non-linear due to their double charm quark content, as reflected by the factor g_c^2 in equation (2). To illustrate the sensitivity of the model predictions on $dN_{c\bar{c}}^{dir}/dy$, we exhibit the results of a 20% variation with respect to the value given in Table 2. The open charm cross section is not yet measured at RHIC. However, some indirect measurements can be well reproduced, within the experimental errors, by PYTHIA calculations using a p-p charm cross sections scaled with the number of collisions N_{coll} of $650 \mu\text{b}$ [50]. The corresponding value at $\sqrt{s_{NN}}=130 \text{ GeV}$ is $330 \mu\text{b}$ [49]. For comparison, the NLO pQCD values we are using [34] are 390 and $235 \mu\text{b}$, respectively. Despite the still large experimental uncertainties, this discrepancy, recognized earlier in ref. [10], needs to be understood. We note that, dependent on the input parameters used in the NLO calculations [34,10], possible variations of the open charm production cross section for the RHIC energy are of the order of $\pm 20\%$. In terms of our model this variation corresponds to about a $\pm 30\%$ change in J/ψ yield which is also centrality dependent (see middle panel in Fig. 4). If we use the PHENIX p-p cross section of $650 \mu\text{b}$, the calculated yield is a factor 2.5 larger for $N_{part}=350$ and increases somewhat stronger with centrality, in disagreement with the data. As apparent in Fig. 4, the predictive power of our model or of any similar model relies heavily on the accurate knowledge of the overall charm production cross section. A simultaneous description of the centrality dependence of open charm together with J/ψ production is, in this respect, mandatory to test the concept of the statistical origin of open and hidden charm hadrons in heavy ion collisions at relativistic energies.

The apparent weak dependence of J/ψ yield on freeze-out temperature, seen in Fig. 4, may be surprising. This is particularly the case since in the thermal model considered in [1] this dependence was shown to be very strong. In our model this result is a consequence of the charm balance equation (2). The temperature variation leads, obviously, to a different number of thermally produced charmed hadrons as in [1], but this is compensated by the g_c factor. The approximate temperature dependence of g_c and the J/ψ yield are:

$$g_c(T) \sim 1/N_D^{th} \sim e^{\frac{m_D}{T}}, \quad N_{J/\psi}(T) = g_c^2 N_{J/\psi}^{th} \sim e^{\frac{2m_D - m_{J/\psi}}{T}} \quad (3)$$

Table 4

Temperature dependence at RHIC, for central collisions.

T	160	170	180	180/160
$dN_{D^+}^{th}/dy$	0.0368	0.0554	0.0775	2.106
$dN_{J/\psi}^{th}/dy$	$0.672 \cdot 10^{-4}$	$0.153 \cdot 10^{-3}$	$0.311 \cdot 10^{-3}$	4.628
g_c	12.85	8.33	5.77	1/2.227
dN_{D^+}/dy	0.415	0.404	0.391	0.942
$dN_{J/\psi}/dy$	0.0111	0.0106	0.0103	0.928
$N_{\psi'}/N_{J/\psi}$	0.031	0.037	0.045	1.452

As a result of the small mass difference in the exponent the J/ψ yield exhibits only a weak sensitivity on T . This is in contrast to the purely thermal case where the yield scales with $\exp(-m_{J/\psi}/T)$. The results are summarized in Table 4, where we present the number of J/ψ and D^+ mesons produced thermally ($N_{J/\psi}^{th}$ and $N_{D^+}^{th}$, respectively) and within the frame of our statistical hadronization model. Also shown are the values of g_c and the yield ratio $\psi'/J/\psi$ for three different values of T . The compensations are evident in the last column of Table 4, where ratios for the two extreme temperatures are calculated. The only exception is the ratio $\psi'/J/\psi$, which is obviously identical in the statistical hadronization scenario and in the thermal model and coincides, for $T \simeq 170$ MeV, with the measured value at SPS [2].

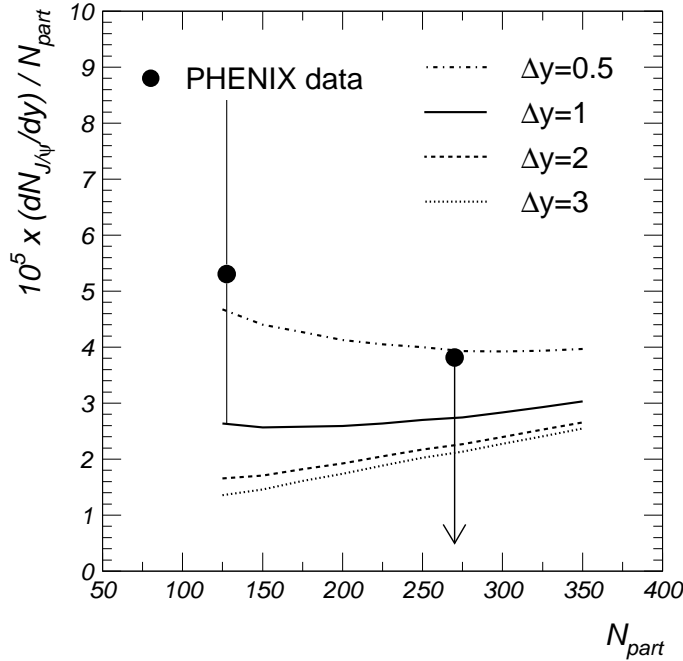


Fig. 5. Centrality dependence of rapidity densities of J/ψ mesons at RHIC for different rapidity window sizes. The lines are calculations, the dots are experimental data from PHENIX collaboration [48] (the point for the central collisions is the upper limit for 90% C.L.).

Most of our results presented above are obtained considering a one unit rapidity window at midrapidity, while results for the full volume were presented only for the SPS. Unlike the kinetic model of Thews et al. [9,10], our model does not contain dynamical aspects of the coalescence process. However, in our approach, the width of the rapidity window does influence the results in the canonical regime. For the grand-canonical case, attained only at LHC energy, there is no dependence on the width of the rapidity window, due to a simple cancellation between the variation of the volume, proportional to the rapidity slice in case of a flat rapidity distribution, and the variation of $N_{c\bar{c}}^{dir}$, also proportional to the width of the rapidity slice. In Fig. 5 we present the centrality dependence of J/ψ rapidity densities for RHIC energy and for different rapidity windows Δy from 0.5 to 3. The dependence on Δy resembles that of the kinetic model [10], but is less pronounced. The available data are not yet precise enough to rule out any of the scenarios considered. However, for the kinetic model [10], the cases of small Δy seem to be ruled out by the present PHENIX data.

We stress in this context that the size of Δy window has a potentially large impact on the results at SPS energy. It is conceivable that no charm enhancement is needed to explain the data if one considers a sufficiently narrow rapidity window for the statistical hadronization.

The results presented above were obtained under the assumption of statistical hadronization of quarks and gluons. In addition, for charm quarks the yields were constrained by the charm balance equation that was formulated in the canonical ensemble. We have further assumed that charm quarks are entirely produced via primary hard scattering and thermalized in the QGP. No secondary production of charm in the initial and final state was included in our calculations. Final state effects like nuclear absorption of J/ψ [51] are also neglected.

4 Conclusions

We have demonstrated that the statistical coalescence approach yields a good description of the measured centrality dependence of J/ψ production at SPS energy, albeit with a charm cross section increased by a factor of 2.8 compared to current NLO perturbative QCD calculations. Rapidity densities for open and hidden charm mesons are predicted to increase strongly with energy, with striking changes in centrality dependence. First RHIC data on J/ψ production support the current predictions, although the experimental errors are for the moment too large to allow firm conclusions. We emphasize that the predictive power of our model relies heavily on the accuracy of the charm cross section, not yet measured in heavy-ion collisions. The statistical coalescence implies travel of charm quarks over significant distances e.g. in a QGP. If the model predictions will describe consistently precision data this would be a clear signal for the presence of a deconfined phase.

Acknowledgments

We acknowledge stimulating discussions with R.L. Thews. K.R. acknowledges the support of the Alexander von Humboldt Foundation (AvH).

References

- [1] M. Gaździcki, M.I. Gorenstein, Phys. Rev. Lett. 83 (1999) 4009 [hep-ph/9905515].
- [2] P. Braun-Munzinger, J. Stachel, Phys. Lett. B 490 (2000) 196 [nucl-th/0007059].
- [3] P. Braun-Munzinger, J. Stachel, Nucl. Phys. A 690 (2001) 119c [nucl-th/0012064].
- [4] M.I. Gorenstein, A.P. Kostyuk, H. Stöcker, W. Greiner, Phys. Lett. B 509 (2001) 277 [hep-ph/0010148].
- [5] L. Grandchamp, R. Rapp, Phys. Lett. B 523 (2001) 60 [hep-ph/0103124].
- [6] M.I. Gorenstein, A.P. Kostyuk, H. Stöcker, W. Greiner, Phys. Lett. B 524 (2002) 265 [hep-ph/0104071].
- [7] A.P. Kostyuk, M.I. Gorenstein, H. Stöcker, W. Greiner, Phys. Lett. B 531 (2002) 195 [hep-ph/0110269].
- [8] L. Grandchamp, R. Rapp, Nucl. Phys. A 709 (2002) 415 [hep-ph/0205305].
- [9] R.L. Thews, M. Schroedter, J. Rafelski, Phys. Rev. C 63 (2001) 054905 [hep-ph/0007323].
- [10] R.L. Thews, hep-ph/0206179.
- [11] T. Matsui, H. Satz, Phys. Lett. B 178 (1986) 416.
- [12] R. Vogt (p. 250c) in S.A. Bass et al., Nucl. Phys. A 661 (1999) 205c.
- [13] F. Karsch, AIP Conf. Proc. 602 (2001) 323, hep-lat/0109017.
- [14] C.Y. Wong, Phys. Rev. Lett. 76 (1996) 196; Erratum *ibid.* 76 (1996) 4987.
- [15] P. Braun-Munzinger, J. Stachel, J. Phys. G 28 (2002) 1971 [nucl-th/0112051].
- [16] M.I. Gorenstein, K.A. Bugaev, M. Gaździcki, Phys. Rev. Lett. 88 (2002) 132301 [hep-ph/0112197].
- [17] S. Batsouli, S. Kelly, M. Gyulassy, J.L. Nagle, Phys. Lett. B 557 (2003) 26 [nucl-th/0212068].
- [18] J. Nagle, nucl-th/0306001.
- [19] Z.W. Lin and D. Molnar, nucl-th/0304045.
- [20] Yu.L. Dokshitzer, D.E. Kharzeev, Phys. Lett. B 519 (2001) 199 [hep-ph/0106202].
- [21] J. Cleymans, K. Redlich, E. Suhonen, Z. Phys. C 51 (1991) 137.

- [22] Review of Particle Physics, Phys. Rev. D 66 (2002) 010001.
- [23] P. Braun-Munzinger, I. Heppe and J. Stachel, Phys. Lett. B 465 (1999) 15.
- [24] P. Braun-Munzinger, D. Magestro, K. Redlich, and J. Stachel, Phys. Lett. B 518 (2001) 41, and references therein.
- [25] NA38 Collaboration, M.C. Abreu et al., Phys. Lett. B 449 (1999) 128.
- [26] NA50 Collaboration, M.C. Abreu et al., Nucl. Phys. A 638 (1998) 261c.
- [27] H. Sorge, E. Shuryak, I. Zahed, Phys. Rev. Lett. 79 (1997) 2775.
- [28] NA49 Collaboration, S.V. Afanasiev et al., Phys. Rev. C 66 (2002) 054902 [nucl-ex/0205002].
- [29] PHOBOS Collaboration, B.B. Back et al., Phys. Rev. Lett. 88 (2002) 022302 [nucl-ex/0108009]; Nucl. Phys. A 715 (2003) 490c [nucl-ex/0211002].
- [30] E877 Collaboration, J. Barrette et al., Phys. Rev. C 51 (1995) 3309 [nucl-ex/9412003].
- [31] NA50 Collaboration, M.C. Abreu et al., Phys. Lett. B 530 (2002) 33.
- [32] BRAHMS Collaboration, I.G. Bearden et al., Phys. Lett. B 523 (2001) 227 [nucl-ex/0108016]; Phys. Rev. Lett. 88 (2002) 202301 [nucl-ex/0112001].
- [33] K.J. Eskola, K. Kajantie, P.V. Ruuskanen, K. Tuominen, Nucl. Phys. B 570 (2000) 379 [hep-ph/9909456]; K.J. Eskola, K. Kajantie, K. Tuominen, Nucl. Phys. A 700 (2002) 509 [hep-ph/0106330].
- [34] R. Vogt, hep-ph/0111271; hep-ph/0203151.
- [35] R. Vogt, Heavy Ion Phys. 9 (1999) 339 [nucl-th/9903051] and refs. therein.
- [36] D. Miśkowiec, <http://www.gsi.de/~misko/overlap/>.
- [37] P. Braun-Munzinger, J. Cleymans, H. Oeschler, K. Redlich, Nucl. Phys. A 697 (2002) 902 [hep-ph/0106066].
- [38] NA50 Collaboration, M.C. Abreu et al., Phys. Lett. B 450 (1999) 456; Phys. Lett. B 477 (2000) 28.
- [39] J. Gosset, A. Baldissieri, H. Borel, F. Staley, Y. Terrien, Eur. Phys. J. C 13 (2000) 63.
- [40] P. Braun-Munzinger and K. Redlich, Eur. Phys. J. C 16 (2000) 519.
- [41] NA50 Collaboration, M.C. Abreu et al., Nucl. Phys. A 698 (2002) 539c.
- [42] C.Y. Wong, Z.Q. Wang, Phys. Lett. B 367 (1996) 50.
- [43] R. Rapp, E. Shuryak, Phys. Lett. B 473 (2000) 13.
- [44] K. Gallmeister, B. Kämpfer, O.P. Pavlenko, Phys. Lett. B 473 (2000) 20 [hep-ph/9908269].
- [45] J.-P. Blaizot, P.M. Dinh, J.-Y. Ollitrault, Phys. Rev. Lett. 85 (2000) 4012 [nucl-th/0007020].
- [46] A. Capella, A. B. Kaidalov, D. Sousa, Phys. Rev. C 65 (2002) 054908 [nucl-th/0105021].

- [47] R.L. Thews, hep-ph/030205.
- [48] S.S. Adler et al., PHENIX Collaboration, nucl-ex/0305030.
- [49] PHENIX Collaboration, K. Adcox et al., Phys. Rev. Lett. 88 (2002) 192303 [nucl-ex/0202002].
- [50] R. Averbeck, PHENIX Collaboration, Nucl. Phys. A 715 (2003) 695c [nucl-ex/0209016].
- [51] M.J. Leitch et al., Phys. Rev. Lett. 84 (2000) 3256 [nucl-ex/9909007].